Turkish Journal of Electrical Engineering & Computer Sciences

http://journals.tubitak.gov.tr/elektrik/

Research Article

Turk J Elec Eng & Comp Sci
(2017) 25: 2513 – 2521

doi:10.3906/elk-1604-341

Investigation of adaptive control of robot manipulators with uncertain features for trajectory tracking employing HIL simulation technique

Senthil Kumar JAGATHEESA PERUMAL[1,*], **Senthil Kumar NATARAJAN**[2]
[1]Department of Electronics and Communication Engineering, Mepco Schlenk Engineering College, Sivakasi, Tamil Nadu, India
[2]Department of Electrical and Electronics Engineering, Mepco Schlenk Engineering College, Sivakasi, Tamil Nadu, India

Received: 25.04.2016 • **Accepted/Published Online:** 20.09.2016 • **Final Version:** 29.05.2017

Abstract: This paper investigates the hardware-in-the-loop (HIL) simulation approach for dynamic control of a three-link rigid robot manipulator that possesses ambiguous dynamics and kinematics. The task with two adaptive control schemes has been realized with the objective of task space trajectory-tracking of the end effector of the robotic manipulator. Both proposed controllers are designed by considering the joint reference velocities and the additional separation property. Based on these, the controllers can be referred to as reference velocity (RV) and reference velocity separation (RVS) adaptive controllers, respectively. The RV adaptive controller can yield better performance with proper alterations, without the cost of conventional gain choice. The HIL simulations are carried out with the aid of a model of three-link rigid robotic manipulator, developed using MATLAB/Simulink, and the RV and RVS adaptive controllers were implemented with the C2000 real-time controller. From the HIL simulation, the performance of the two adaptive controllers is analyzed for task space tracking of the robotic manipulator.

Key words: Robot manipulators, adaptive controllers, reference velocity, separation property, hardware-in-the-loop simulation

1. Introduction

As a robotic system design requires multidisciplinary mastering, partitioning the design tasks into various subsystems simplifies their analysis and synthesis. Therefore, utilizing the real hardware modules in the loop of a real-time simulation enables a detailed analysis of sensor noises and actuator limitations of robotic systems. This can be accomplished with the hardware-in-the-loop (HIL) technique, where the control algorithms are implemented in the actual hardware, rather than utilizing the simulated model. This kind of HIL-based simulation modeling supports rapid prototyping of control algorithms [1]. Various fuzzy-based adaptive controllers were proposed by various researchers [2–4]. There are also various other proposed techniques for the control of robotic manipulators, based on feedback linearization, computed torque control, variable structure compensator, etc. [5]. Adaptive control of actuators of robotic manipulators has also been carried out, combining a proportional-integral-derivative (PID) and variable structure compensator to improve the precision of trajectory tracking [6]. However, the lack of real hardware implementation of the control algorithm makes the robotic manipulator tolerate precision in control appliances. As robotic manipulators employed in the task

*Correspondence: senthilkumarj@mepcoeng.ac.in

space may undergo kinematic uncertainties, adaptive control schemes are mandatory. The adaptive regional feedback control strategy, based on Jacobian feedback and inverse Jacobian feedback control, is employed to overcome the stability issues of dynamics and kinematic uncertain systems [7,8]. The performance criteria in task space are accurate trajectory tracking and better transient response, which are considered to be lacking in those techniques.

This paper presents a solution by realizing two different adaptive control schemes with the objective of task space trajectory-tracking of the end effector of the robotic manipulator. The joint reference velocities of the manipulator are taken into account for both the proposed controllers and the design of the second controller includes an additional separation property. To test the robustness of the proposed adaptive controllers, the HIL simulation approach is employed. The control algorithms are implemented in the real hardware. The actuators and dynamics of the robotic manipulator are designed as a portion of the simulator system, rather than investing in an actual robotic manipulator [9]. The first reference velocity (RV) controller improves the performance with better trajectory tracking for the robotic manipulator. With the expense of conservative gain selection, the RV adaptive controller can handle the dynamic and kinematic uncertainties of the robotic manipulator. The joint serving module of the second reference velocity separation (RVS) adaptive controller can be modified with joint velocity commands with the aid of the separation property. Jacobian feedback control is not suitable for this issue due to the coupling nature in the torque input to the robotic manipulator due to adaptive transpose Jacobian feedback and a lack of quick adaptation [10].

2. Dynamics and kinematics of the robotic manipulator

A three-link planar serial robotic manipulator placed on a fixed base plane is shown in Figure 1. The three revolute joints $\mathbf{J_1}$, $\mathbf{J_2}$, and $\mathbf{J_3}$ are driven by separate actuators and the rotating angles of these three links are θ_1, θ_2, **and** θ_3, respectively. From the Euler–Lagrangian formulation, the dynamic equations of the robotic manipulator are derived, which describe the relationship between joint motion, accelerations, and torque [11,12]. The dynamic equation of motion of an $'\mathbf{n}'$ link robotic manipulator with rotary joints is given in joint space, described by Lagrangian dynamics as:

$$\mathbf{M}(\theta)\ddot{\theta}+\mathbf{C}\left(\theta,\dot{\theta}\right)\dot{\theta}+\mathbf{G}(\theta)=\tau, \quad (1)$$

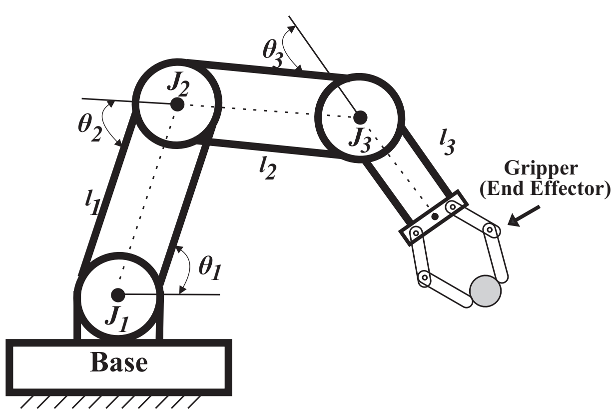

Figure 1. Model of the robotic manipulator.

where $\mathbf{M}(\theta) \in \mathbf{R}^{\mathbf{n}\times\mathbf{n}}$ is the inertia matrix of the manipulator, θ is the n × 1 joint position vector, $\mathbf{C}\left(\theta,\dot{\theta}\right) \in \mathbf{R}^{\mathbf{n}\times\mathbf{n}}$ is the matrix of centrifugal and Coriolis forces, $\mathbf{G}(\theta) \in \mathbf{R}^{\mathbf{n}}$ is the vector of gravitational torque, and $\tau \in \mathbf{R}^{\mathbf{n}}$ is the vector of joint actuator torques. The modeling of the chosen manipulator is performed with three rigid links, the first connecting joints $\mathbf{J_1}$ and $\mathbf{J_2}$ represented with the length of $\mathbf{l_1}$, the second connecting joints $\mathbf{J_2}$ and $\mathbf{J_3}$ represented with the length of $\mathbf{l_2}$, and the last link connecting joint $\mathbf{J_3}$ and the gripper represented with the length of $\mathbf{l_3}$.

The torque vector for the actuators of those three links can be expressed as:

$$\tau = [\tau_{\mathbf{1}}\, \tau_{\mathbf{2}}\, \tau_{\mathbf{3}}]^{\mathbf{T}}, \tag{2}$$

where $\tau_{\mathbf{1}}$, $\tau_{\mathbf{2}}$, and $\tau_{\mathbf{3}}$ are torques applied to the actuators of joints $\mathbf{J_1}\, \mathbf{J_2}$, **and** $\mathbf{J_3}$, respectively. Eqs. (1) and (2) show the controller output torques. Representing the position of the end effector in Cartesian task space as $\mathbf{x} \in \mathbf{R}^{\mathbf{n}}$, by nonlinear mapping the joint position can be given as:

$$\mathbf{x} = \mathbf{f}(\theta), \tag{3}$$

where $\theta \in \mathbf{R}^{\mathbf{n}}$ represents the joint position and $\mathbf{f}: \mathbf{R}^{\mathbf{n}} \to \mathbf{R}^{\mathbf{n}}$ is the mapping from joint to task space. The relation between joint space velocity and task space velocity can be obtained by differentiating Eq. (3) with respect to the time as represented by Eq. (4):

$$\dot{x} = \mathbf{J}(\theta)\,\dot{\theta}, \tag{4}$$

where $\mathbf{J}(\theta) \in \mathbf{R}^{\mathbf{n}\times\mathbf{n}}$ is the Jacobian matrix. With the direct kinematics given in Eq. (4), we cannot predict the task space position and velocity unless the kinematic parameters are known. The kinematics depend on a constant parameter vector $\mathbf{a_k}$ and follow the linearity in parameters property. Here we assume the task space sensors to be potentiometers or a camera employed to give the position and velocity information in the task space [13].

3. Design of adaptive controllers using HIL technique

Due to complex nonlinearities and uncertain parameters, the usage of deterministic control methods is quite challenging [14]. Additionally, to overcome the drawbacks of passivity-based controllers, inverse dynamics controllers are employed [15]. Here we investigate the adaptive controller implementation for a robotic manipulator with uncertain dynamics and kinematics with the aid of the HIL simulation technique by taking into account the actuator dynamics [16]. We consider the control objective as the driving of the robot manipulator end effector to track the desired trajectory $\mathbf{x_d}$ asymptotically in the task space [17]. It is also assumed that the translational velocity $\dot{x}_{\mathbf{d}}$ and acceleration $\ddot{x}_{\mathbf{d}}$ of the desired trajectory for the task space are all bounded by considering the bounded nature of the actuators [18].

3.1. Design of reference velocity adaptive controller

The joint RV $\dot{\theta}_r$ is considered as the basic parameter of choice for the design of the RV adaptive controller. This algorithm estimates the parameters online, which appear in the dynamic model of the robotic manipulator [19]. It is used to derive the control law to control the actuators in the joints of the robotic manipulator. To overcome the drawbacks of the velocity measurements, the sliding observer design technique can be used to estimate the joint velocities [20]. The design illustration of the RV adaptive controller that was implemented using the C2000 real-time controller is shown in Figure 2. The joint reference for the RV adaptive controller velocity is represented using the estimated Jacobian matrix as:

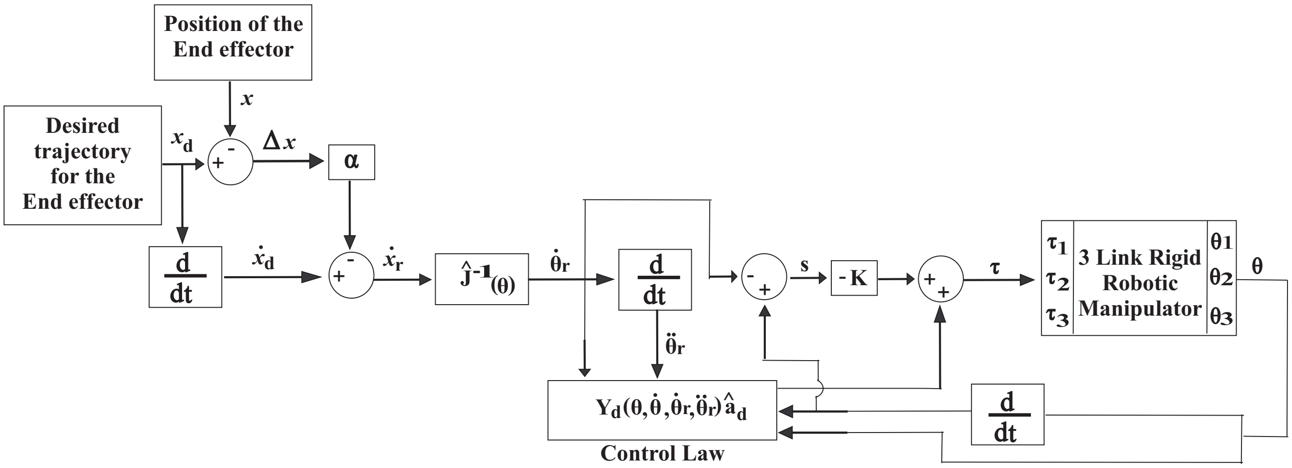

Figure 2. Block diagram of RV controller using HIL for a three-link robotic manipulator.

$$\dot{\theta}_r = \hat{J}^{-\mathbf{1}}(\theta)\,\dot{x}_{\mathbf{r}}, \tag{5}$$

where $\dot{x}_{\mathbf{r}} = \dot{x}_{\mathbf{d}} - \alpha\mathbf{\Delta x}$ is the position tracking error with respect to the task space of the robotic manipulator, α is a positive design constant, and $\hat{J}^{-\mathbf{1}}(\theta)$ is the inverse of the estimated Jacobian matrix obtained with the estimate of $\mathbf{a_k}$ represented as $\hat{a}_{\mathbf{k}}$ for $\mathbf{J^{-1}}(\theta)$ [21]. The joint reference acceleration of the links can be obtained by differentiating Eq. (5) with respect to time:

$$\ddot{\theta}_{\mathbf{r}} = \hat{J}^{-\mathbf{1}}(\theta)\left[\ddot{x}_{\mathbf{r}} - \dot{\hat{J}}(\theta)\,\dot{\theta}_{\mathbf{r}}\right]. \tag{6}$$

By defining the sliding vector as $\mathbf{s} = \dot{\theta} - \dot{\theta}_r$, it can also be written as:

$$\mathbf{s} = \mathbf{J^{-1}}(\theta)\left[\dot{x} - \mathbf{J}(\theta)\,\dot{\theta}_r\right], \tag{7}$$

$$\mathbf{s} = \mathbf{J^{-1}}(\theta)\left[\mathbf{\Delta}\dot{x} + \alpha\mathbf{\Delta x} + \mathbf{Y_k}\left(\theta,\dot{\theta}_r\right)\mathbf{\Delta a_k}\right]. \tag{8}$$

This can be further written in terms of tracking error as:

$$\mathbf{\Delta}\dot{x} = -\alpha\mathbf{\Delta x} - \mathbf{Y_k}\left(\theta,\dot{\theta}_r\right)\mathbf{\Delta a_k} + \mathbf{J}(\theta)\,\mathbf{s}, \tag{9}$$

where $\mathbf{\Delta a_k} = \hat{a}_{\mathbf{k}} - \mathbf{a_k}$ is the kinematic parameter estimation error. Based on the position, velocity, acceleration, and estimated parameters, the control law can be written as:

$$\tau = -\mathbf{Ks} + \mathbf{Y_d}\left(\theta,\dot{\theta},\dot{\theta}_{\mathbf{r}},\ddot{\theta}_{\mathbf{r}}\right)\hat{a}_{\mathbf{d}}, \tag{10}$$

where $\mathbf{K} \in \mathbf{R^{n\times n}}$ represents a symmetric matrix that is positive and definite. The adaptation laws were formulated by taking into account the dynamic model of the robotic manipulator [20]. The dynamic parameter estimate $\hat{a}_\mathbf{d}$ is updated by:

$$\dot{\hat{a}}_d = -\mathbf{\Gamma_d Y_d^T}\left(\theta,\dot{\theta},\dot{\theta}_\mathbf{r},\ddot{\theta}_\mathbf{r}\right)\mathbf{s}. \tag{11}$$

The estimated kinematic parameter $\hat{a}_\mathbf{k}$ is updated with the help of direct adaptation law as:

$$\dot{\hat{a}}_k = \mathbf{\Gamma_k Y_k^T}\left(\theta,\dot{\theta}_\mathbf{r}\right)\left[(\beta/\alpha)\mathbf{\Delta x} + \mathbf{\Delta x}\right], \tag{12}$$

where $\mathbf{\Gamma_d}$, $\mathbf{\Gamma_k}$ represents a symmetric and positive definite matrix and $\beta \in [\mathbf{0},\mathbf{1}]$ is a design constant. Substituting the control law from Eq. (10) into the dynamics, Eq. (1) yields:

$$\mathbf{M}(\theta)\,\dot{s} + \mathbf{C}\left(\theta,\dot{\theta}\right)\mathbf{s} = -\mathbf{Ks} + \mathbf{Y_d}\left(\theta,\dot{\theta},\dot{\theta}_\mathbf{r},\ddot{\theta}_\mathbf{r}\right)\mathbf{\Delta a_d}, \tag{13}$$

where $\mathbf{\Delta a_d} = \hat{a}_\mathbf{d} - \mathbf{a_d}$. The closed loop robotic manipulator system controlled using the RV adaptive controller can be described by Eqs. (9) and (13). The corresponding adaptation laws are given in Eqs. (11) and (12).

3.2. Design of reference velocity separation adaptive controller

In this section, we present the design strategy followed for the RVS adaptive controller, which has a separation property and uses a different joint reference velocity and kinematic parameter adaptation law. The implementation of the RVS adaptive controller in the C2000 real-time controller is shown in Figure 3. The joint reference for the RVS adaptive controller velocity $\dot{\theta}_r$ is represented using the estimated Jacobian matrix as:

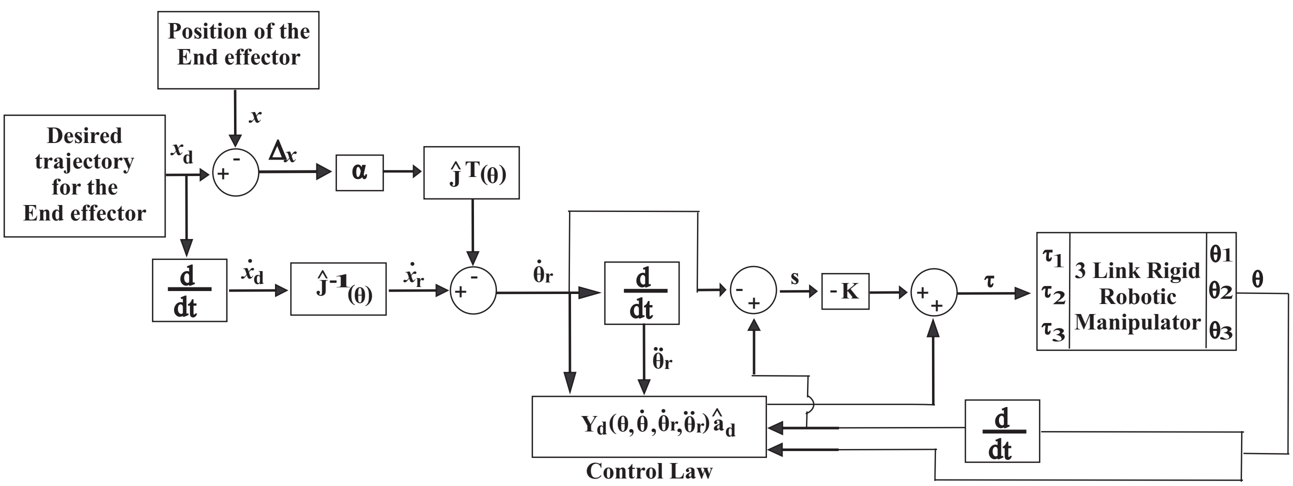

Figure 3. Block diagram of RVS controller using HIL for a three-link robotic manipulator.

$$\dot{\theta}_r = \dot{x}_r - \hat{J}^T(\theta)\,\alpha\Delta x\,, \tag{14}$$

where the derivation of position tracking error is given as $\dot{x}_r = \hat{J}^{-1}(\theta)\,\dot{x}_d$. The closed loop robotic manipulator system is then described for the RVS adaptive controller by Eqs. (13) and (15):

$$\Delta\dot{x} = -\alpha\hat{J}^T(\theta)\,\hat{J}(\theta)\,\Delta x - Y_k\left(\theta,\dot{\theta}_r\right)\Delta a_k + \hat{J}(\theta)\,s. \tag{15}$$

The control law for the RVS adaptive controller and the adaptation law are the same as that of the RV adaptive controller, represented by Eqs. (10) and (11). However, the kinematic parameter adaptation law for the RVS adaptive controller is given as:

$$\dot{\hat{a}}_k = \Gamma_k Y_k^T \left(\theta, \dot{\theta}\right) \Delta x. \tag{16}$$

4. Performance of the HIL-simulated adaptive controllers

The two designed adaptive control schemes, RV and RVS, were implemented with the C2000 real-time controller, and the HIL simulations were carried out using MATLAB 2012b and Code Composer Studio 5. They were implemented to actuate a three-link planar rigid robotic manipulator that clutches an unknown object. The link lengths of the chosen manipulator are $l_1 = 0.09$ m, $l_2 = 0.063$ m, and $l_3 = 0.115$ m and the corresponding masses of the links are $m_1 = 0.15$ kg, $m_2 = 0.1$ kg, and $m_3 = 0.28$ kg. The sampling period is chosen as 5 ms and the desired trajectory of the end effector of the manipulator is chosen as $x_d = [1.6755 + 0.3 \cos \pi t,\ 3.9952 + 0.3\, sin\, \pi t]^T$. For the RV adaptive controller, the controller parameters are chosen as $K = 30$, $\alpha = 10$, $\beta = 0.5$, $\Gamma_d = 200$, $and\, \Gamma_k = 300$, respectively. The actual values of the parameter estimates are selected as $a_d = [7.9627, -0.9601,\ 19.2827,\ 10.1496]^T$ and

$a_k = [2.0000,\ 3.3855,\ 0.8001]^T$. The HIL simulation results for the RV adaptive controller tracking errors for joints $J_1\ J_2\ and\ J_3$ are shown in Figure 4 and the torques for the corresponding joints are shown in Figure 5.

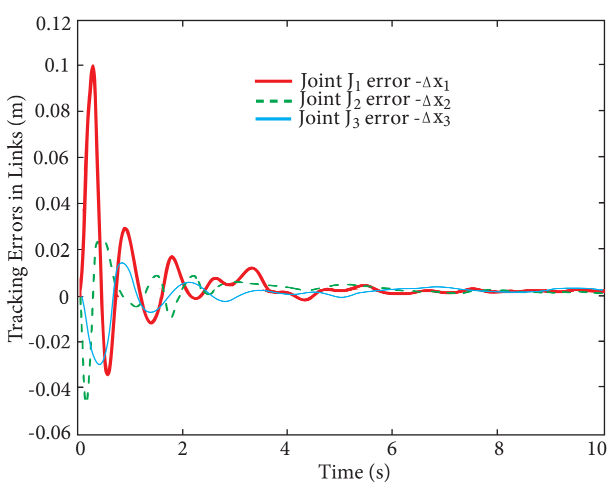

Figure 4. Tracking errors of the position of three joints while moving the end effector using RV adaptive controller.

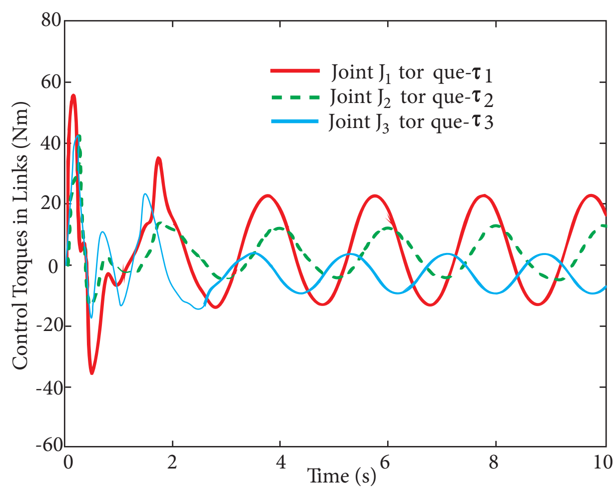

Figure 5. Torques applied to the three joints for moving the end effector using RV adaptive controller.

For the RVS adaptive controller, the controller parameters are chosen to be the same as those of the RV controller, except for the design parameter $\alpha = 1.5$, since the equivalent feedback gain contains the transpose of the estimated Jacobian matrix.

The HIL simulation results for the RVS adaptive controller for tracking errors and torques of the joints are plotted in Figures 6 and 7, respectively. From the simulation results, it is obvious that the RV adaptive controller results in a better tracking accuracy of approximately 0.0015 at $t = 6$ s and more adequate utilization of the joint torques. The tracking accuracy under the RVS adaptive controller after $t = 6$ s is analogous; hence, the closed-loop dynamics are approximate to a linear dynamics that are critically damped, and the other parameters are chosen to be the same as those in the RV adaptive controller.

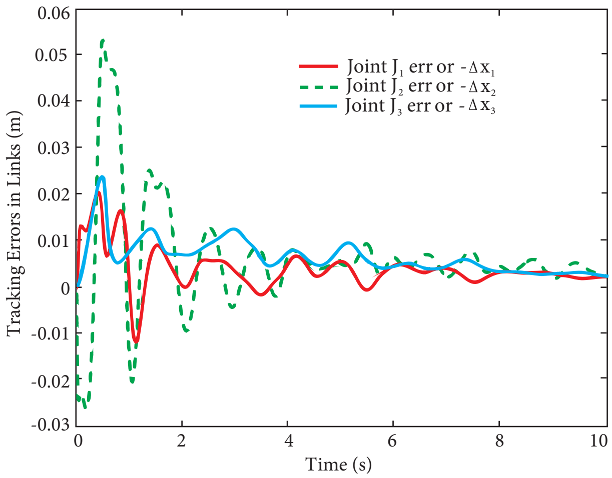

Figure 6. Tracking errors of the position of three joints while moving the end effector using RVS adaptive controller.

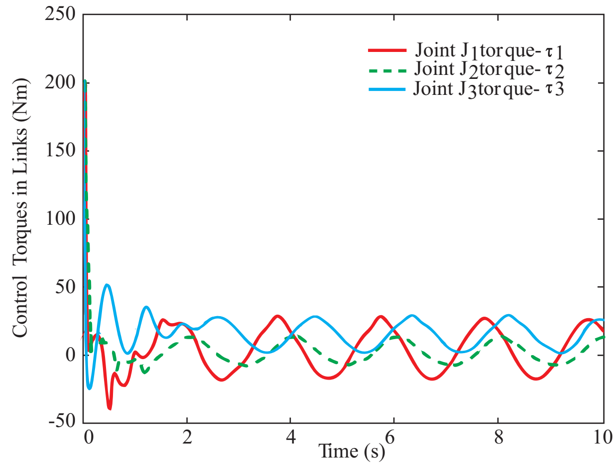

Figure 7. Torques applied to the three joints for moving the end effector using RV adaptive controller.

Tables 1 and 2 list the comparison of errors and torques, respectively, at the three joints of the robotic manipulator for the proposed controllers. They are tabulated for time samples of a 1-s delay, and the equivalent average of the errors and torques is consolidated in Table 3.

Table 1. Comparison of tracking errors in the position of three joints for RV and RVS adaptive controllers at a time sample of 1 s.

Time (s)	Joint J_1 error (m)		Joint J_2 error (m)		Joint J_3 error (m)	
	RV	RVS	RV	RVS	RV	RVS
1	0.0022	0.0009	0.0032	0.0162	0.0097	0.0082
2	0.0036	0.0001	0.0047	0.0083	0.0060	0.0071
3	0.0074	0.0034	0.0065	0.0013	0.0001	0.0123
4	0.0019	0.0060	0.0043	0.0079	0.0012	0.0080
5	0.0029	0.0057	0.0055	0.0050	0.0003	0.0093
6	0.0015	0.0051	0.0026	0.0063	0.0033	0.0048
7	0.0024	0.0041	0.0019	0.0024	0.0040	0.0051
8	0.0029	0.0033	0.0032	0.0042	0.0021	0.0035
9	0.0026	0.0027	0.0019	0.0021	0.0033	0.0031
10	0.0023	0.0022	0.0015	0.0026	0.0030	0.0025

It is obvious from Tables 1 and 3 that the tracking and average errors of the joints are lower for the RV adaptive controller. From Tables 2 and 3 it is also evident that the RVS adaptive controller uses more torque to actuate the joints. The main advantage of the RVS adaptive controller lies in the responses of the joint tracking errors, which become more uniform. The tracking errors converge quickly compared to the RV controller using constant gain feedback, as shown in Figure 4.

5. Conclusion

In this paper, we have considered the adaptive tracking of the end effector of a robot manipulator that is subjected to both dynamic and kinematic uncertainties. The proposed adaptive controllers, with different

Table 2. Comparison of applied torques for RV and RVS adaptive controllers to the three joints at a time sample of 1 s.

Time (s)	Joint J_1 torque (Nm)		Joint J_2 torque (Nm)		Joint J_3torque (Nm)	
	RV	RVS	RV	RVS	RV	RVS
1	5.9505	1.4239	1.7677	2.9183	12.8865	11.3871
2	13.0881	19.0142	11.4314	13.0799	8.3887	20.7942
3	8.3696	8.3298	4.7097	6.3640	2.5466	15.1397
4	15.6813	14.7987	11.7913	13.3904	5.9808	16.7264
5	8.0329	8.0155	4.3110	6.9169	1.3772	10.0878
6	16.0058	15.7422	11.8793	13.3994	8.7560	22.0056
7	7.8270	8.9515	4.2566	6.5996	3.4649	4.7816
8	16.2033	16.2766	12.6296	13.6186	9.1256	26.4928
9	7.7353	8.3865	4.7384	7.0572	2.4216	4.1001
10	16.8000	17.2417	12.8082	9.5049	7.1881	25.8490

Table 3. Average response of joint errors and torques using RV and RVS adaptive controllers.

	Joint J_1		Joint J_2		Joint J_3	
	RV	RVS	RV	RVS	RV	RVS
Average joint error (m)	0.0030	0.0033	0.0035	0.0056	0.0033	0.0064
Average joint torque (Nm)	11.5694	11.8181	8.0323	9.2849	6.2136	15.7364

reference velocity and additional separation property, are employed to solve the trajectory-tracking problem of the end effector with better precision. Our experimentation, based on HIL simulation using the C2000 controller, also suggests that a good tracking performance can be obtained in the task space of the end effector with the aid of RV and RVS adaptive controllers. However, a valuable feature of the proposed adaptive control schemes is the separation of the kinematic and dynamic loops. The kinematic control law, represented by the joint reference velocity and the kinematic adaptation law, ensures the convergence of the tracking errors in task space. The joint velocity tracking error of the proposed adaptive controllers is bounded and square-integrable. From the HIL-implemented experimental results, it is obvious that the designed RV adaptive controller possesses better trajectory-tracking accuracy with minimum torque and the RVS adaptive controller responds better to joint tracking errors and converges faster.

References

[1] Pouria S, Samereh Y. State of the art: hardware in the loop modelling and simulation with its applications in design, development and implementation of system and control software. J Dyn Control Syst 2015; 3: 470-479.

[2] Khalate A, Leena G, Ray G. An adaptive fuzzy controller for trajectory tracking of robot manipulator. Lect Notes Contr Inf 2011; 2: 364-370.

[3] Psillakis HE, Alexandridis AT. Adaptive neural motion control of n-link robot manipulators subject to unknown disturbances and stochastic perturbations. IEE P-Contr Theor Ap 2006; 153: 127-138.

[4] Xie J, Liu GL, Yan SZ, Xu WF, Qiang WY. Study on neural network adaptive control method for uncertain space manipulators. Chinese J Aeronaut 2010; 31: 123-129.

[5] Iqbal J, Islam RU, Khan MF. Control strategies for robotic manipulators. In: IEEE 2012 International Conference on Robotics and Artificial Intelligence; 22–23 October 2012; Rawalpindi, Pakistan. New York, NY, USA: IEEE. pp. 26-33.

[6] Jingmei Z, Haiyang, H, Kang B. Studies of adaptive control methods based on VSC for trajectory tracking of robotic manipulators. In: IEEE 2012 International Conference on Robotics and Biomimetics; 11–14 December 2012; Guangzhou, China. New York, NY, USA: IEEE. pp. 429-434.

[7] Tsai CC, Hung CC, Chang CF. Trajectory planning and control of a 7-DOF robotic manipulator. In: IEEE 2014 International Conference on Advanced Robotics and Intelligent Systems; 6–8 June 2014; Taipei, Taiwan. New York, NY, USA: IEEE. pp. 78-84.

[8] Li X, Cheah CC. Adaptive regional feedback control of robotic manipulator with uncertain kinematics and depth information. In: IEEE 2012 American Control Conference; 27–29 June 2012; Montreal, Canada. New York, NY, USA: IEEE. pp. 5472-5477.

[9] Guo Y, Zhou F, Marian N, Angelov CK. Hardware-in-the-loop simulation of component-based embedded systems. In: SEFI 2007 International Workshop on Research and Education in Mechatronics; 14–15 June 2007; Tallinn, Estonia. Leuven, Belgium: European Society for Engineering Education. pp. 268-273.

[10] Hovakimyan N, Cao C. Output feedback. In: Hovakimyan N, Cao C, editors. L1 Adaptive Control Theory: Guaranteed Robustness with Fast Adaptation. Philadelphia, PA, USA: Society for Industrial and Applied Mathematics, 2010. pp. 179-207.

[11] Merlet JP, Pierrot F. Modelling of parallel robots. In: Dombre E, Khalil W, editors. Robot Manipulators Modeling: Performance Analysis and Control. London, UK: ISTE, 2007. pp. 81-133.

[12] Sciavicco L, Siciliano B. Dynamics. In: Sciavicco L, Siciliano B, editors. Modelling and Control of Robot Manipulators. London, UK: Springer, 2000. pp. 131-183.

[13] Mahyuddin MN, Khan SG, Herrmann G. A novel robust adaptive control algorithm with finite-time online parameter estimation of a humanoid robot arm. Robot Auton Syst 2014; 62: 294-305.

[14] Morikazu T, Suguru A. An adaptive trajectory control of manipulators. Int J Control 1981; 34: 219-230.

[15] Wang H, Xie Y. Adaptive inverse dynamics control of robots with uncertain kinematics and dynamics. Automatica 2009; 45: 2114-2119.

[16] Salimi KY, Namvar M. Adaptive control of robot manipulators including actuator dynamics and without joint torque measurement. In: IEEE 2010 International Conference on Robotics and Automation; 3–7 May 2010; Anchorage, AK, USA. New York, NY, USA: IEEE. pp. 4639-4644.

[17] Guo Q, Perruquetti W, Efimov D. Universal robust adaptive control of robot manipulators using real time estimation. In: IFAC 2015 Conference on Modelling, Identification and Control of Nonlinear Systems; 24–26 June 2015; Saint Petersburg, Russia. Laxenburg, Austria: IFAC. pp. 499-504.

[18] Lopez-Araujo DJ. Adaptive control of robot manipulators with bounded inputs. PhD, Potosino Institute of Scientific and Technological Research A.C., San Luis Potosí, Mexico, 2013.

[19] Craig JJ, Hsu P, Sastry SS. Adaptive control of mechanical manipulators. Int J Robot Res 1987; 6: 16-28.

[20] Liang X, Huang X, Wang M, Zeng X. Adaptive task-space tracking control of robots without task-space- and joint-space-velocity measurements. IEEE T Robot 2010; 26: 733-742.

[21] Bennehar M, Chemori A, Pierrot F. A new extension of desired compensation adaptive control and its real-time application to redundantly actuated PKMs. IEEE 2014 International Conference on Intelligent Robots and Systems; 14–18 September 2014; Chicago, IL, USA. New York, NY, USA: IEEE. pp. 1670-1675.